



## **Influence of Electrode Distance on Electrical Energy Production of Microbial Fuel Cell using Tapioca Wastewater**

**Ardiyan Harimawan<sup>\*</sup>, Hary Devianto, Rd. Habib R. M. T. Al-Aziz, Dian Shofinita & Tjandra Setiadi**

Department of Chemical Engineering, Faculty of Industrial Technology, Institut Teknologi Bandung, Jalan Ganesa No. 10 Bandung 40132, Indonesia

\*E-mail: ardiyan@che.itb.ac.id

**Abstract.** The microbial fuel cell (MFC) is an alternative technology that can be used to simultaneously solve problems related to wastewater production and energy demand. This study investigates the influence of electrode distance on power density in a microbial fuel cell using tapioca wastewater. A graphite sheet without metal catalyst was used for both electrodes, separated by a Nafion membrane. Four variations of electrode distance were used. The MFC with the longest electrode distance achieved the highest equilibrium OCV (676 mV), while the MFC with the shortest electrode distance achieved the highest power density (7.74 mW/m<sup>2</sup>). Electrochemical impedance spectroscopy (EIS) measurement suggested that the charge transfer resistance was dominant in all MFC configurations. The wastewater COD removal was in the range of 35-46%, which is in accordance with the power density of MFCs.

**Keywords:** *COD removal; electrode distance; microbial fuel cell; power density; tapioca wastewater.*

### **1 Introduction**

The growing world population will cause several major problems, including an increase in energy demand and waste production. The microbial fuel cell is one of the potential solutions for the energy as well as waste problem, since it can utilize microorganisms in wastewater to directly produce a beneficial product, i.e. electricity.

In a microbial fuel cell (MFC), microorganisms are used as catalyst to oxidize organic or inorganic material, and directly generate electricity [1,2]. An MFC generally consists of two chambers, namely an anode chamber and a cathode chamber, separated by proton exchange membranes. In the anode chamber, microorganisms oxidize the organic or inorganic matter and produce electrons and protons, while in the cathode chamber, the electrons and protons react with a catholyte or oxygen to form water. The anode and cathode are connected by a wire containing an electrical device to change the electrons into electricity [3].

The microorganisms used in MFCs are exoelectrogen bacteria, which can transfer electrons outside the cell to the anode as electron acceptors [4]. The anode chamber is usually operated in anaerobic condition to avoid oxygen, while the cathode chamber is in aerobic condition because the electrochemical reaction requires oxygen as the final electron acceptor [5].

The electrons produced by microorganisms are transferred to the anode and the cathode via a conductive wire. The electrons are transferred through an electrical device, such as a resistor or battery, which transforms it into electricity [6]. Carbon is the material that is usually used for the electrode in MFCs. A graphite sheet is a carbon-based electrode that is cheaper than other carbon-based electrodes, but can still maintain good conductivity. The anode and cathode chambers can be separated by a semipermeable membrane, which acts as a bridge for the protons to be transferred from the anode to the cathode chamber. This membrane can also inhibit the movement of oxygen from the cathode to the anode. Thus, the MFC can simultaneously treat wastewater and produce electricity, providing a potential alternative energy source for the future [2].

Tapioca wastewater can be used as a substrate in an MFC. In Indonesia, from one ton of tapioca production, about 40-60 m<sup>3</sup> of tapioca wastewater is produced. The COD value of this wastewater is in the range of 7000 and 30,000 mg/L, depending on various factors, such as process location, type of cassava, and also type and amount of water used [7]. Based on the Indonesian Ministry of Environment and Forestry Regulation Number 5 Year 2014 on the standard quality of wastewater for the tapioca industry, the maximum COD that can be discharged into the environment is 300 mg/l. Hence, further treatment of the wastewater is required.

The main challenge in the development of an MFC is obtaining optimal performance. One solution is using platinum catalyst at the electrode [8]. However, the cost of platinum catalyst is very high. Thus, further study regarding the use of a low-cost method to increase MFC performance, such as using appropriate electrode types or varying electrode distance, should be explored [9-12].

Previous studies have reported that better performance of MFCs, quantified by power density, was found when the distance between the electrodes was reduced [9-12]. Hence, it is important to find the optimum distance to provide higher power density, as well as to explain the dominant resistance during mass and charge transfers in the MFC. Furthermore, the use of tapioca wastewater as a substrate together with a graphite sheet as the electrode with a membrane to separate electrodes (membrane electrode assembly, or MEA) has not been much

explored. Thus, the aims of this study were: to investigate the use of tapioca wastewater and a graphite sheet electrode without metal catalyst in an MFC; to determine the influence of electrode distance on MFC performance and COD removal efficiency; and to investigate the effect of resistance in MFC operation.

## **2 Materials and Methods**

### **2.1 Substrate and Inoculum**

Tapioca wastewater [7] with the following characteristics was used as the substrate: COD 3,200 mg/L, total nitrogen 58 mg/L, total phosphate 7.3 mg/L, and pH 4.0. The wastewater was prepared before the experiment at a sufficient amount for the whole experiment and was stored in the refrigerator to maintain its characteristics. Rumen feces from a biogas installation were used as inoculum source. The inoculum was acclimated in the tapioca wastewater until the mixed liquor suspended solid (MLSS) was constant at around 3,000 mg/L.

### **2.2 MFC Configuration**

A series of MFCs was made from acrylic material with a width of 0.6 cm, consisting of an anode chamber and a cathode chamber with a volume size of approximately  $8 \times 6 \times 5 \text{ cm}^3$ . The chambers were separated by a Nafion 202 membrane, which was adhered with electrode or without electrode, depending on the MFC variation. The material of the electrodes was graphite sheet without metal catalyst. The size of the electrodes was  $3 \times 2 \text{ cm}^2$ .

The distance between the electrodes was varied in this study. The configurations used in the experiments were: (1) MFC-MEA (both electrodes adhered without distance and separated by a membrane); (2) MFC-2 (electrodes separated by a membrane with the distance between the electrodes at 2 cm and the distance between the electrode and the membrane at 1 cm); (3) MFC-AM (anode and membrane adhered together and separated from the cathode by a distance of 1 cm); and (4) MFC-KM (cathode and membrane adhered together and separated from the anode by a distance of 1 cm).

### **2.3 MFC Preparation**

The experiments were conducted at room temperature, pH 7 and inoculum concentration of 60-80 mg/L. The nitrogen gas was purged into the anode chamber to provide an anaerobic condition and agitation for the inoculum. An aerial pump was used to pump air into the cathode chamber, which contained phosphate buffer pH 7 and 100 ppm  $\text{KMnO}_4$  as catholyte.

## 2.4 MFC performance Characterization

Five analysis were conducted in this study to characterize the performance of the MFC: (1) a potentiodynamic analysis to measure the maximum current and voltage generated by the MFC, (2) electrochemical impedance spectroscopy (EIS) to model the resistances that occur in the MFC, (3) scanning electron microscopy (SEM) and Fourier transform infra-red (FTIR) spectroscopy to observe the morphology and composition of the biofilm formed on the anode, and (5) X-ray diffraction (XRD) to investigate the transformation of the electrode material before and after operation of the MFC.

## 3 Results and Discussion

### 3.1 Open Circuit Voltage (OCV)

The open circuit voltage (OCV) is the potential difference between the MFC electrodes without any connected external load. The results from the OCV measurement with electrode distance variation are shown in Figure 1. This figure shows that the highest equilibrium voltage was found for MFC-2.

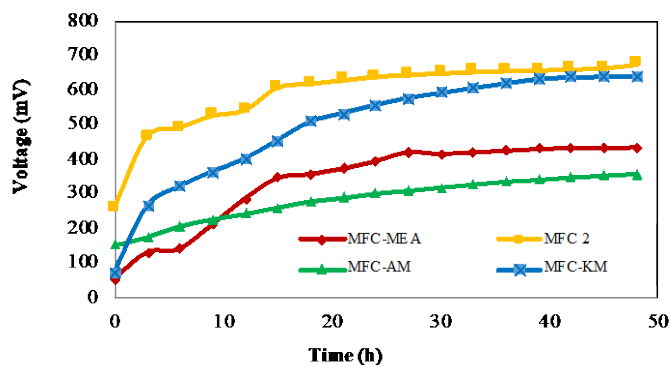


**Figure 1** Open circuit voltage (OCV) measurements for different electrode distances.

The increasing trend of voltage during the initial process showed the adaptation of the bacteria to produce the enzymes that are used in the electron transfer process from the bacteria to the anode. All variations showed constant voltages after 30 hours. This result indicates that after 30 hours, the bacteria were adapted and were able to transfer electrons to the anode [13]. The highest equilibrium OCV values were found for MFC-2 (672 mV) and MFC-KM (639 mV). This may due to the distance between the anode and the membrane, providing a larger surface area in MFC-2 and MFC-KM compared to MFC-

MEA and MFC-AM. This larger surface area may lead to a higher rate of bacteria growth on the anodes, hence a higher production of protons and electrons was achieved. Furthermore, a larger surface area of the anode may cause higher potential reduction.

The highest equilibrium OCV values found in this study were lower than those from another study [14]. It was reported that the ideal cell voltage cannot be predicted because the electrons transferred from the substrate to the anode pass through the respiration system, which may vary for each bacteria [3]. Thus, the cell voltage depends on the growth condition of the bacteria.

### 3.2 Potentiodynamic

The voltage decreased and the current density increased as a higher load was given to the MFC series. When a load was given to the MFC series, the protons and electrons moved to the cathode via the membrane and the external circuit wire, respectively. Figure 2 shows the results of the potentiodynamic measurement. A lower slope of the curve indicates a lower resistance in the MFC series.

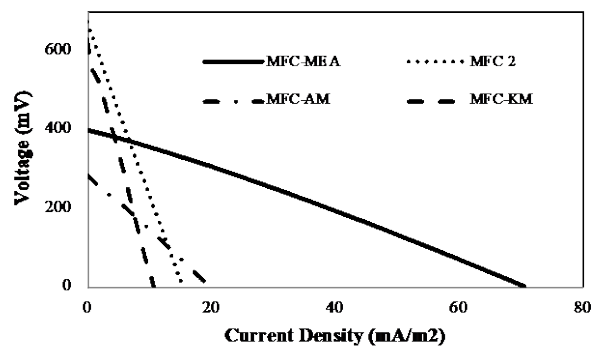


Figure 2 Polarization curve for different electrode distances.

Figure 2 shows that the MFC-MEA series had the lowest slope, giving the lowest resistance of all series. This resistance is dominated by ohmic and mass transport resistance. Ohmic resistance occurs when protons move to the cathode through the membrane and electrons move to the cathode through the external circuit. Mass transport resistance occurs when the reactant or product at the anode does not have a high enough concentration to move protons to the cathode through the membrane, which can limit the reaction rate in the MFC process. This results corroborates the outcomes of other studies, proving that decreasing the electrode distance is one of the possible solutions to decrease the ohmic resistance [15].

### 3.3 Power Density

The power ( $P$ ) can be calculated using the current and voltage data from the potentiodynamic measurement with Eq. (1):

$$P = I \cdot E_{MFC} \quad (1)$$

In Eq. (1),  $P$  is power (Watt),  $I$  is current (A) and  $E_{mfc}$  is voltage (V). The power calculated from Eq. (1) does not indicate the efficiency of the MFC series because the surface area of the anode may also influence the power density of the MFC. Hence, the power density value with consideration of the surface area of the anode ( $A_{anode}$ ) for the MFC series, was calculated using Eq. (2):

$$P = \frac{I \cdot E_{MFC}}{A_{anode}} \quad (2)$$

Besides the power density, the potentiodynamic measurement can also provide values of the current at maximum power attained by the MFC series, as shown in Figure 3. The values of the power density and the current at the maximum power attained by all MFC series are given in Table 1. Table 1 shows that the highest maximum power density was achieved by MFC-MEA due to the small distance between its electrodes. This small distance may lead to better transfer of electrons and protons from the bacteria to the anode or from the anode to the cathode due to the smaller ohmic resistance. Previous studies have also reported that higher power density was achieved when there was no distance between the anode and the cathode, which were only separated by membranes (Table 2). Table 2 shows a comparison of the power density obtained in this study with previous studies, where the power density in this study was found to be lower ( $7.74 \text{ mW/m}^2$ ). This may due to the absence of catalyst, hindering optimum degradation of wastewater in the anode chamber.

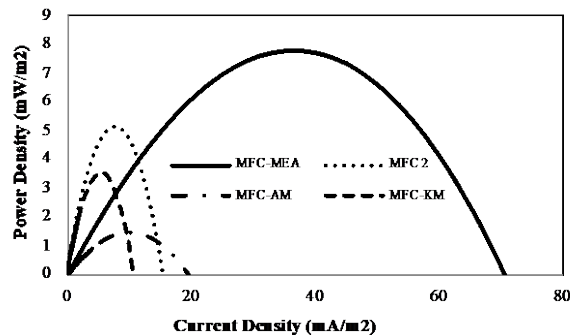


**Figure 3** Power density and current density curve at maximum power for different electrode distances.

**Table 1** Power density and current at maximum power for different electrode distances.

Parameter	MFC-MEA	MFC-2	MFC-AM	MFC-KM
P (mW/m <sup>2</sup> )	7.74	2.55	1.45	1.77
I at Pmax (mA/m <sup>2</sup> )	21.92	9.26	6.44	6.70

**Table 2** Previous studies on membrane electrode assembly.

Anode	Cathode	Membrane	Power Density (mW/m <sup>2</sup> )	Authors
Carbon sheet	Carbon sheet + Pt	<i>Nafion</i> 117	600	[16]
Carbon sheet	Carbon sheet + Pt	<i>Nafion</i> 115	1180	[15]
Graphit rod	Graphit rod + Pt	<i>Nafion</i> 117	57.5	[17]
Graphit rod	Graphit rod + Pt	<i>Non-woven Filter</i>	97	
<i>Graphite sheet</i>	<i>Graphite sheet</i> without catalyst	<i>Nafion</i> 212	7.74	This research

Previous studies have found that a smaller distance between the anode and the cathode will result in higher power density [9-12]. However, in this study, the MFC-2 series with longer electrode distance than MFC-KM and MFC-AM gave higher power density. This may be due to the effect of proton or ion diffusion at the electrode being adhered to the membrane in MFC-KM and MFC-AM, which is able to inhibit the electron and proton transfer. This diffusion may also have occurred in the MFC-KM series because there may have been some protons carried by the wastewater in the anode chamber and by the KMnO<sub>4</sub> solution in the cathode chamber.

Proton or ion diffusion may also have occurred in MFC-2, where the anode and cathode were separated. However, since the membrane was not adhered to the electrode, the performance of the membrane may have been higher, hence providing effective transfer of protons from the anode to the cathode.

### 3.4 Electrochemical Impedance Spectroscopy (EIS)

The types of resistance phenomena in all MFC series in this study can be explained particularly by using electrochemical impedance spectroscopy (EIS). There are three resistances that can be observed by this measurement. The initial area is ohmic resistance, the middle area is ion or charge resistance, and the third area is a mass resistance indicator. The frequency of this EIS measurement was set between 100 kHz and 1 mHz [18]. The impedance measurement in this research is represented by the Nyquist plot in Figure 4. Figure 4 shows that MFC-2 and MFC-KM gave higher resistance in a similar

trend as the polarization curve. When a gap is present between the anode and the membrane, protons that are generated by the bacteria cannot move directly to the membrane. Thus, the protons will be carried by the wastewater in the anode chamber.

This figure also shows that the shortest resistance was found for MFC-MEA. This may be due to the short distances between anode, membrane, and cathode so that the ohmic (and other) resistance decreased. Such small resistance values may result in more effective proton and electron transfer. Figure 4 also shows that mass transfer resistance was observed for MFC-AM and MFC-KM. This result indicates that when only one part of the electrodes is adhered to the membrane, a diffusion process that increases mass transport resistance may occur.

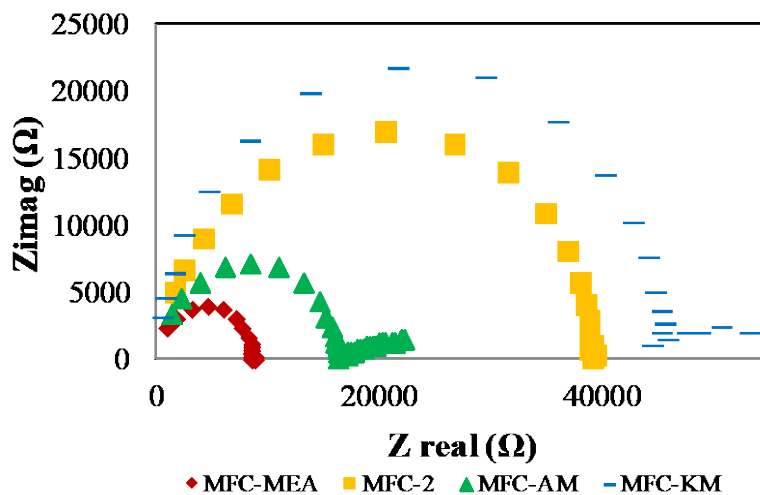


**Figure 4** Nyquist plot for different electrode distances.

The internal resistance value can then be determined by the curve of EIS measurement, which requires fitting of the Nyquist curve. The fitting or modeling requires an equivalent circuit model for all MFC series [18].

The equivalent circuit model for this study is shown in Figure 5. The internal resistance values for all MFC series that were found in this study are shown in Table 3. The internal resistance values found in this study appear to be high, which suggests that the system can still be improved, particularly regarding the chamber system, microorganism type and other factors that can inhibit operation process.



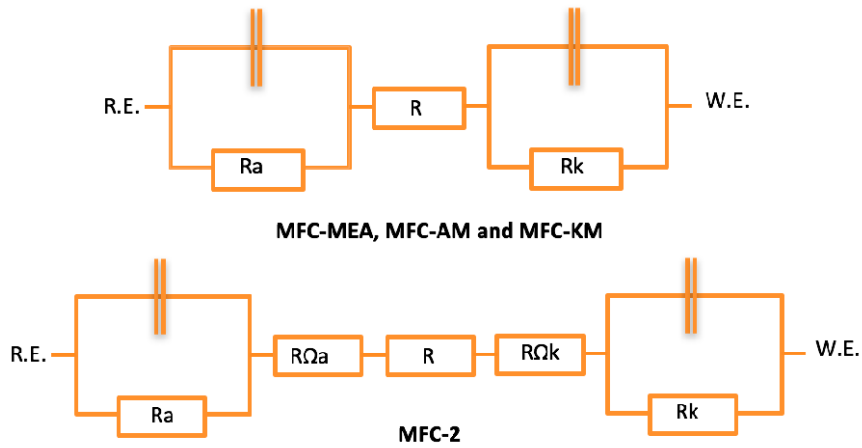


**Figure 5** Equivalent circuit model for different electrode distances.

**Table 3** Internal resistance value for different electrode distances.

Resistance	MFC-MEA	MFC-2	MFC-AM	MFC-KM
<b>Ra (KΩ)</b>	8.26	30.0	14.57	44.4
<b>Rk (KΩ)</b>	0.015	8.38	1.33	3.15

### 3.5 Characterization of Electrode Material

The characterization of the electrode material before and after the MFC process aims to observe the influence of biofilm formation on the electrode’s surface, especially on the anode, to see whether there are any changes in the material structure of the anode due to bacterial growth. The graphite sheet that was used for the electrodes in this research had carbon contents of about 99.8%. A previous study found that the XRD measurement peak for graphite can be detected at  $2\theta$  positions  $26.5\text{-}26.6^\circ$  and  $54.5\text{-}54.7^\circ$  [19]. The result of XRD analysis of this study (Figure 6) shows two main XRD peaks, which were observed at  $2\theta$  positions  $26.45^\circ$  and  $54.52^\circ$  (for the initial electrode before MFC operation), and  $26.58^\circ$  and  $54.68^\circ$  (for the electrode after MFC operation). These peaks were observed at similar positions as for graphite that is reported in the literature.

The level at which the biofilm changes the material of the anode can be estimated by the crystallite size, which can be determined using the Scherrer formula (Eq. (3)). In Eq. (3),  $L$  is the average crystal size (nm);  $K$  is the Scherrer constant (0.94);  $\lambda$  is the wavelength, which depends on the anode that is used for the analysis (1.54 nm in this study, because Cu was used);  $B$  (radian)

is the maximum peak from the diffraction result measurement (full width at half maximum, or FWHM); and  $\theta$  is the Bragg angle ( $^{\circ}$ ) at the diffraction peak.

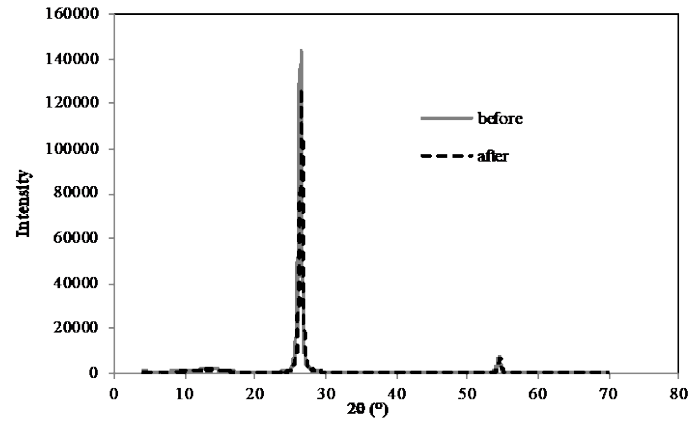


**Figure 6** XRD analysis result of electrode material before and after MFC operation.

$$L = \frac{k\lambda}{B \cdot \cos \theta} \quad (3)$$

The result of the crystal size of the graphite sheet for this study is shown in Table 4. This result shows that there was no significant effect of the microbial metabolism on the carbon electrode, specifically based on the crystal size of the graphic sheet.

**Table 4** Crystal size of graphite sheet before and after MFC operation.

	2 $\theta$	FWHM	$\theta$ ( $^{\circ}$ )	$\theta$ (rad)	cos $\theta$	L (nm)
<b>Before</b>	26.444	0.409	13.224	0.230	0.973	3.635
	54.515	0.53	27.257	0.475	0.888	3.072
<b>After</b>	26.584	0.443	13.292	0.231	0.973	3.357
	54.685	0.538	27.342	0.477	0.888	3.028

### 3.6 Biofilm Characterization

The matrix of the biofilm structure generally consists of 97% water, 2-5% microbe cells, 3-6% EPS or extracellular polymeric substances and ions. Extracellular polymeric substances or EPS can be hydrophilic or hydrophobic and consist of about 40-95% polysaccharide and 1-60% proteins, 1-10% nucleic acid and 1-40% lipids [4, 20]. The biofilm structure observed from FTIR is shown in Figure 7. In this figure, the band at 2922.16  $\text{cm}^{-1}$  and 2854.85  $\text{cm}^{-1}$

shows a functional group of fatty acid membrane and some amino acids, which is similar to previous reports [21]. In addition, the peak at  $1656.85\text{ cm}^{-1}$  indicates a C=O bond in the protein amide band. The same peak was also detected as an N-H group as a component of an extracellular polymeric substance. Deformation of the C-H group at the  $=\text{CH}_2$  functional group was detected at the peaks of  $1448.54\text{ cm}^{-1}$  and  $1383.96\text{ cm}^{-1}$ . Vibration stretching of the carboxyl group or C-N group was observed at the peak of  $1085.92\text{ cm}^{-1}$ . The characterization of biofilm morphology on the anode's surface was observed by scanning electron microscopy (SEM). Figure 8 shows an image of the anode's surface covered by biofilm before and after MFC operation for all MFC series.

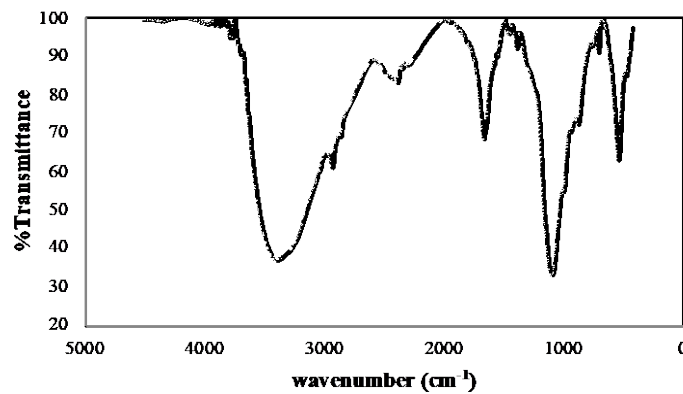


**Figure 7** Biofilm FTIR spectrum for all MFC series.

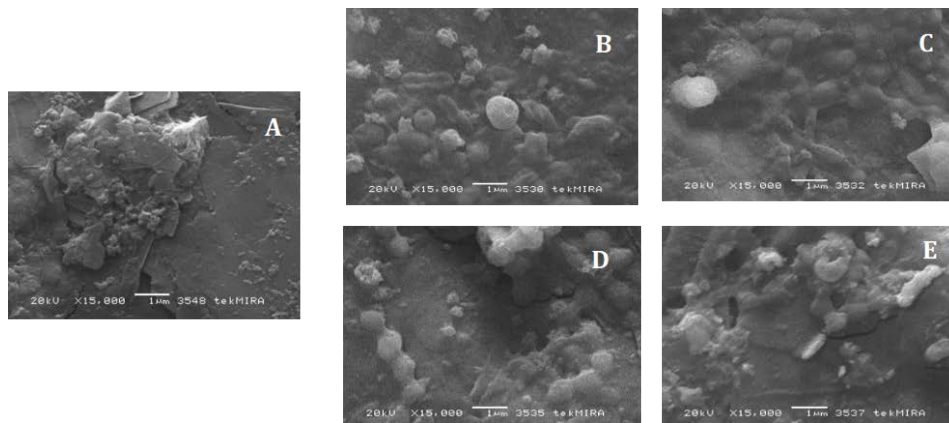


**Figure 8** Image of the biofilm surface area before and after MFC operation: (A) initial MFC, (B) MFC-MEA, (C) MFC-2, (D) MFC-AM, (E) MFC-KM.

Biofilm at the MFC anode can decrease the resistance at the anode and increase the current density of the MFC [22]. The performance of an MFC depends not only on the thickness of the biofilm formed on the anode's surface, but also on the condition at the anode, the type of bacteria or substrate used for MFC operation.

### 3.7 COD Removal Efficiency

Besides generating electricity, an MFC can also be used for treating wastewater. One of the wastewater indicators is chemical oxygen demand (COD). COD removal efficiency can be determined by comparing the COD values before and after MFC operation. A higher COD removal efficiency indicates higher wastewater potential to be used for MFC operation. The COD removal efficiency found in this research was in the range of 35-46%. MFC-MEA had the highest COD removal efficiency, while MFC-AM showed the lowest efficiency. Table 5 shows the COD removal efficiencies of all MFC series.

**Table 5** COD removal efficiency before and after MFC operation for different electrode distances.

	MFC-MEA	MFC-2	MFC-AM	MFC-KM
<b>COD before operation (mg/l)</b>	4160	4160	4160	4160
<b>COD after operation (mg/l)</b>	2240	2320	2720	2560
<b>Δ COD removal (mg/l)</b>	1920	1840	1440	1600
<b>COD removal efficiency (%)</b>	46.15	44.23	34.62	38.46

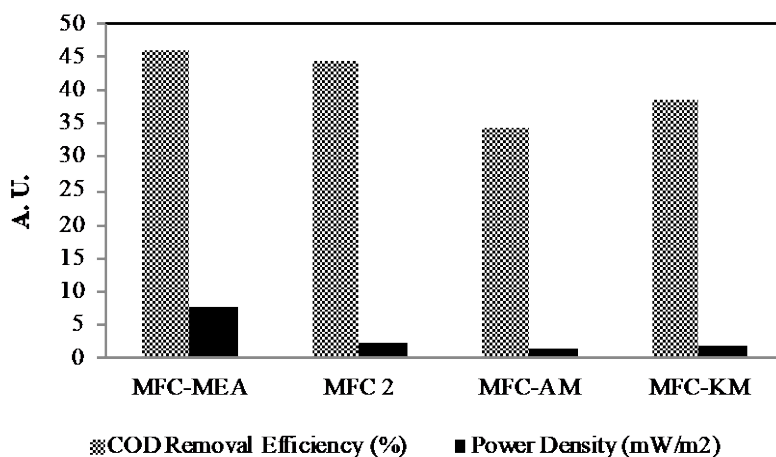


**Figure 9** COD removal efficiency and power density for different electrode distances.

Oxidation of wastewater in MFC produces electrons and protons. The higher the bacterial growth at the anode, the higher the probability of electrons and protons being generated by the bacteria, hence affecting MFC performance. It has been reported that higher COD removal efficiency is correlated with a higher current generated by the MFC [23]. Figure 9 shows that the COD removal efficiency value was proportional to the power density for all MFC series, showing similar trends as in other studies [23].

#### 4 Conclusions

The effect of electrode distance on the electrical production in a microbial fuel cell (MFC) using tapioca wastewater was investigated in this study. Four variations of electrode distance were observed: MFC-MEA (anode and cathode adhered together and Nafion membrane separating the electrode), MFC-2 (distance from anode to cathode at 2 cm), MFC-AM (anode adhered to the membrane with distance from the cathode at 1 cm), and MFC-KM (cathode adhered to the membrane with distance from the anode at 1 cm). It was found that tapioca wastewater and graphite sheet without metal catalyst can be used as MFC components. MFC-2 was found to produce the highest open circuit voltage equilibrium (676 mV), while MFC-MEA was found to produce the highest power density (7.74 mW/m<sup>2</sup>). Furthermore, the electrochemical impedance spectroscopy measurement suggested that the charge transfer resistance was dominant in all MFC configurations, while the mass transfer resistance was dominant only in MFC-AM and MFC-KM. MFC-MEA performed better than the other configurations because it had low internal resistance, while the lowest MFC performance was found for MFC-AM and MFC-KM due to the presence of mass transport resistance. The COD removal efficiency was found to be 35-46 %, which is proportional to the increase in the power density for all MFCs.

#### Acknowledgement

This work was supported under the P3MI ITB (Program Penelitian, Pengabdian kepada Masyarakat, dan Inovasi Institut Teknologi Bandung) funding scheme.

#### References

- [1] Ahn, Y. & Logan, B.E., *Effectiveness of Domestic Wastewater Treatment using Microbial Fuel Cells at Ambient and Mesophilic Temperatures*, *Bioresource Technology*, **101**(2), pp. 469-475, 2010.
- [2] Min, B. & Logan, B.E., *Continuous Electricity Generation from Domestic Wastewater and Organic Substrates in a Flat Plate Microbial*

- Fuel Cell*, Environmental Science & Technology, **38**(21), pp. 5809-5814, 2004.
- [3] Du, Z., Li, H. & Gu, T., *A State of the Art Review on Microbial Fuel Cells: A Promising Technology for Wastewater Treatment and Bioenergy*, Biotechnology Advances, **25**(5), pp. 464-482, 2007.
- [4] Logan, B.E., Hamelers, B., Rozendal, R., Schröder, U., Keller, J., Freguia, S., Aelterman, P., Verstraete, W. & Rabaey, K., *Microbial Fuel Cells: Methodology and Technology*, Environmental Science & Technology, **40**(17), pp. 5181-5192, 2006.
- [5] Lovley, D.R., *Bug Juice: Harvesting Electricity with Microorganisms*, Nature Reviews Microbiology, **4**(7), pp. 497, 2006.
- [6] Reddy, L.V., Kumar, S.P. & Wee, Y-J., *Microbial Fuel Cells (MFCs) – A Novel Source of Energy for New Millennium*, Current Research Technology and Education Topics in Applied Microbiology and Microbial Biotechnology, **2**(13), pp. 956-964, 2010.
- [7] Setyawaty, R., Katayama-Hirayama, K., Kaneko, H. & Hirayama, K., *Current Tapioca Starch Wastewater (TSW) Management in Indonesia*, World Appl Sci J, **14**, pp. 658-665, 2011.
- [8] Trinh, N.T., Park, J.H. & Kim, B-W., *Increased Generation of Electricity in a Microbial Fuel Cell using Geobacter Sulfurreducens*, Korean Journal of Chemical Engineering, **26**(3), pp. 748-753, 2009.
- [9] Ghangrekar, M.M. & Shinde, V.B., *Performance of Membrane-less Microbial Fuel Cell Treating Wastewater and Effect of Electrode Distance and Area on Electricity Production*, Bioresource Technology, **98**(15), pp. 2879-2885, 2007.
- [10] Jain, R., Tiwari, D., Sharma, S. & Mishra, P., *Efficiency and Stability of Carbon Cloth Electrodes for Electricity Production from Different Types of Waste Water using Dual Chamber Microbial Fuel Cell*, Journal of Scientific & Industrial Research, **74**, pp. 308-314, 2015.
- [11] Jang, J.K., Pham, T.H., Chang, I.S., Kang, K.H., Moon, H., Cho, K.S., & Kim, B.H., *Construction and Operation of a Novel Mediator- and Membrane-less Microbial Fuel Cell*, Process Biochemistry, **39**(8), pp. 1007-1012, 2004.
- [12] Sangeetha, T. & Muthukumar, M., *Influence of Electrode Material and Electrode Distance on Bioelectricity Production from Sago-processing Wastewater using Microbial Fuel Cell*, Environmental Progress & Sustainable Energy, **32**(2), pp. 390-395, 2013.
- [13] Liu, H., Cheng, S. & Logan, B.E., *Power Generation in Fed-batch Microbial Fuel Cells as a Function of Ionic Strength, Temperature, and Reactor Configuration*, Environmental science & technology, **39**(14), pp. 5488-5493, 2005.
- [14] Logan, B.E., *Microbial Fuel Cells*, John Wiley & Sons, Inc., Hoboken, NJ, United States, 2008.

- [15] Liang, P., Huang, X., Fan, M-Z., Cao, X-X. & Wang, C., *Composition and Distribution of Internal Resistance in Three Types of Microbial Fuel Cells*, Applied Microbiology and Biotechnology, **77**(3), pp. 551-558, 2007.
- [16] Prakash, G.S., Viva, F.A., Bretschger, O., Yang, B., El-Naggar, M. & Neelson, K., *Inoculation Procedures and Characterization of Membrane Electrode Assemblies for Microbial Fuel Cells*, Journal of Power Sources, **195**(1), pp. 111-117, 2010.
- [17] Choi, S., Kim, J.R., Cha, J., Kim, Y., Premier, G.C. & Kim, C., *Enhanced Power Production of a Membrane Electrode Assembly Microbial Fuel Cell (MFC) using a Cost Effective Poly[2,5-benzimidazole] (ABPBI) Impregnated Non-woven Fabric Filter*, Bioresource Technology, **128**, pp. 14-21, 2013.
- [18] Sekar, N. & Ramasamy, R.P., *Electrochemical Impedance Spectroscopy for Microbial Fuel Cell Characterization*, Journal of Microbial Biochemical Technology, **6**(2), pp. 2013.
- [19] Yu, X. & Qiang, L., *Preparation for Graphite Materials and Study on Electrochemical Degradation of Phenol by Graphite Cathodes*, Advances in Materials Physics and Chemistry, **2**(02), pp. 63, 2012.
- [20] Costerton, J.W., Lewandowski, Z., Caldwell, D.E., Korber, D.R. & Lappin-Scott, H.M., *Microbial Biofilms*, Annual Reviews in Microbiology, **49**(1), pp. 711-745, 1995.
- [21] Baranitharan, E., Khan, M.R., Yousuf, A., Teo, W.F.A., Tan, G.Y.A. & Cheng, C.K., *Enhanced Power Generation using Controlled Inoculum from Palm Oil Mill Effluent-fed Microbial Fuel Cell*, Fuel, **143**, pp. 72-79, 2015.
- [22] Zhang, L., Zhu, X., Li, J., Liao, Q. & Ye, D., *Biofilm Formation and Electricity Generation of a Microbial Fuel Cell Started Up under Different External Resistances*, Journal of Power Sources, **196**(15), pp. 6029-6035, 2011.
- [23] Gonzalez del Campo, A., Lobato, J., Cañizares, P., Rodrigo, M.A. & Fernandez Morales, F.J., *Short-term Effects of Temperature and COD in a Microbial Fuel Cell*, Applied Energy, **101**, pp. 213-217, 2013.